

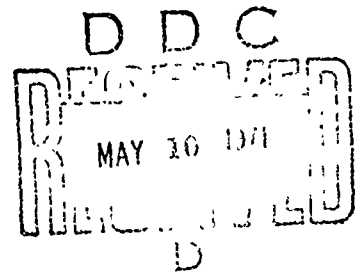
AD 722784

# ON THE STRUCTURE OF PRESSURED SEA ICE

Austin Kovacs

September 1970

DISTRIBUTION STATEMENT A  
Approved for public release;  
Distribution Unlimited



PREPARED FOR  
U.S. COAST GUARD  
BY  
CORPS OF ENGINEERS, U.S. ARMY  
**COLD REGIONS RESEARCH AND ENGINEERING LABORATORY**  
HANOVER, NEW HAMPSHIRE

Reproduced by  
**NATIONAL TECHNICAL  
INFORMATION SERVICE**  
Springfield, Va. 22151

ON THE STRUCTURE OF PRESSURED SEA ICE

by

Austin Kovacs

September 1970

Prepared for  
U.S. Coast Guard  
by

CORPS OF ENGINEERS, U.S. ARMY  
COLD REGIONS RESEARCH AND ENGINEERING LABORATORY  
HANOVER, NEW HAMPSHIRE 03755

## Preface

This report presents findings on the geometry of pressure-related sea ice structures as obtained by conventional surveying and sonar profiling techniques.

The report was prepared by the U.S. Army Cold Regions Research and Engineering Laboratory, for the U.S. Coast Guard, under MIPR NO. Z-70099-02553 dated 23 December 1969.

The study was conducted by Mr. Austin Kovacs, Research Civil Engineer, of the Foundations and Materials Research Branch (Mr. F.E. Crory, Chief), Experimental Engineering Division (Mr. K.A. Linell, Chief). The field work was performed by Mr. John Kalafut of USACRREL and the author. The assistance rendered by Dr. L. Breslau, LCDR J. McIntosh and Chief C. Barger of the U.S. Coast Guard during the field study is greatly appreciated.

## CONTENTS

	Page
Preface-----	ii
Introduction-----	1
Study areas-----	6
Bering and Chuckchi Sea Profile Sites-----	6
Beaufort Sea Profile Site-----	7
Profiling techniques-----	8
Profiles-----	9
Discussion-----	16
Conclusion-----	23
References-----	24

## ILLUSTRATIONS

Figure		
1.	Finger rafting in thin sea ice-----	26
2.	Rafting of sea ice in excess of one meter thick-----	27
3.	Sketch of finger rafting in which both participating sheet has sheared-----	28
4.	Sketch of rafting in which only one participating sheet has sheared-----	28
5.	Long sinuous ridge observed in the Polar Pack-----	29
6.	Extensive hummocking in sea ice east of Pt. Barrow, Alaska	29
7.	View of a rectangular hummock field observed at the Arctic Circle in the Chuckchi Sea north of the Bering Strait	30
8.	Large rampart of grounded sea ice west of Prince of Wales Shoal, Alaska-----	32
9.	Large rampart of grounded sea ice west of Prince of Wales Shoal, Alaska-----	32
10.	Ground view of ice rampart shown in Figure 9-----	33
11.	Large cross-shaped island of grounded ice east of Herschel Island, Canada-----	34
12.	Shear ridge formation along the fast ice / pack ice boundary northeast of Barrow, Alaska-----	34
13.	Shear ridge formation near the boundary of a large floe and fractured ice in the Bering Sea-----	35
14.	Location of the Bering (A) and Chuckchi Sea (B) profile sites-----	36
15.	Raft formations in the Bering Sea-----	37
16.	Raft formation in the Chuckchi Sea north of the Bering Strait in the area of the Arctic Circle-----	38
17.	Rafting and rippling in thin sea ice, Chuckchi Sea-----	39
18.	Rarefied ice conditions in the Chuckchi Sea near the Arctic Circle on 13 March 1970-----	40
19.	Rarefied ice conditions north of the Bering Strait at the Arctic Circle on 13 March 1970-----	41

CONTENTS (Cont'd)

ILLUSTRATIONS (Cont'd)

Figure	Page
20. Aerial view of ridge studied southwest of Lost River, Alaska-----	42
21. Aerial view of the best <u>Northwind</u> and the surrounding sea ice scene on 21 March 1970-----	42
22. Ice conditions along the port side of the beset <u>Northwind</u>	43
23. Plan view of <u>Northwind</u> and the location of Profiles A and B-----	43
24. Ice conditions off the bow of the beset <u>Northwind</u> on 19 March 1970-----	44
25. General location map (a) and area view of the Herschel Island study site (b)-----	45
26. Rarefaction and compaction patterns in winter ice north of the Yukon Territory, Canada-----	46
27. Sea ice conditions east of Herschel Island. The arrow points to ridge study area-----	46
28. Aerial view of ridge line studied off Herachel Island-	47
29. Sonar record obtained during contour measurement of the upper keel portion of Profile 2B-----	48
30. North face of Profile 1 ridge showing variation in thickness of incorporated ice blocks-----	49
31. South face of Profile 1 ridge-----	49
32. Profile 1-----	50
33. Ice conditions off the port side of the beset <u>Northwind</u> on 19 March 1970-----	51
34. Structure of ice block terrain in front of the <u>Northwind</u> on 19 March 1970. Photo was taken near station 25 M as shown on Figure 23-----	51
35. Profile 2A-----	52
36. Profile 2B-----	53
37. Profile 3-----	53
38. Area view of the Profile 3 and 4 study site-----	54
39. Profile 4-----	54
40. View of the <u>Northwind</u> in a rarefied ice field bursting its way through a 2-m-high ridge and fracturing a flce in its path-----	55
41. Rarefied ice conditions around the <u>Northwind</u> on 13 March 1970-----	55
42. Aerial view of the <u>Northwind</u> backed off from a ridge site it could not penetrate after more than an hour of ramming-----	56
43. Ship view of ice-clogged channel and the 2-m-high ridge the <u>Northwind</u> attempted to penetrate-----	56
44. Plankton (dark areas) incorporated in sea ice blocks--	57

## ON THE STRUCTURE OF PRESSURED SEA ICE

By Austin Kovacs

### INTRODUCTION

From the early voyages of tiny square-rigged Greek galleys around 300 B.C. (Zukriegel, 1935) to the most recent voyages of modern, powerful steel icebreakers, man has tried to penetrate the irregular and formidable ice cover of the arctic seas. Man's reasons for venturing into these ice-sheathed waters are varied and many. They include the search for new lands, shorter commerce routes, natural resources and scientific knowledge. Although the arctic is truly a fascinating part of the world, rich in natural resources, beauty, and problems to be solved, the ice cover of the arctic regions still remains the major barrier to exploration and economic development.

Sea ice is one of the world's more complex materials (Sater, 1963). It is nonhomogeneous and anisotropic. It is a conglomerate of freshwater crystals interlaced with pockets of brine and air which have formed between the crystals and crystal plates. These component parts are never in equilibrium but change slowly with time. As a result the physical properties of sea ice are not constant. They are, however, primarily dependent upon temperature and salinity, which in turn are related to the growth history of the ice.

Sea ice near shore is in one sense an extension of land as it remains quasi-immobile during the winter. However, offshore the ice canopy is in perpetual motion, slowly twisting, turning, breaking into smaller pieces, compacting and rarefying. The drift of the ice canopy is an extremely complex resultant of a combination of factors. These include wind stress, water stress, coriolis force, tidal force, atmospheric pressure gradients, internal ice stress and resistance, boundary layer conditions and tilt gradient. It has, however, been long recognized that ice drift is dependent primarily upon wind stress and secondly upon water stress (Arctowski, 1908). The overall effect of these forces is a continuously changing canopy density, i.e. compaction in one area, rarefaction in another and the separation of the ice canopy into floes of endless shapes and sizes.

Large floes under way contain an enormous amount of potential energy. When one of these floes impinges upon another flow or weaker ice unable to resist the contact pressure developed, deformation commonly occurs. The result is one or a combination of deformation structures which give the canopy its rough and often formidable appearance. These structures can be broadly categorized as rafted, ridged, hummocked or shear formations.

Rafting is an interesting phenomenon often associated with thin ice up to 15 cm thick (Figure 1), but also occurring in ice in excess of 1 m thick (Figures 2a and 2b). As Weeks and Kovacs (1970) state, "... there appear to be two different variations of this type of overthrust." In the classic case the two participating sheets shear and

interlock as fingers (Figure 3; after Volkov, 1967) whereas in the second case shearing occurs in only one participating sheet (Figure 4; after Weeks and Anderson, 1958). The corner angles of these thrust structures are often 90 degrees in "thin" ice (Figure 1) but as Anderson and Marljar (1969) state, the thrust lobes become more and more rounded as the thickness of the participating sheets increases (Figures 2a and 2b). Bending strains associated with the rafting of "thick" ice sheets invariably result in fracturing of the rafted lobes as shown in Figure 2a. Often the fractured ice mounds up in front of the advancing lobe. As a result, from a ship it is often difficult to distinguish whether the mound of ice ahead outlines the front of a thrust structure or is a pressure ridge.

A pressure ridge is an accumulation of ice blocks which protrudes both above and below the abutting ice floes. As previously stated, when two floes collide or squeeze together, great pressures can develop at points of contact. If the ice in either or both of the participating floes is unable to resist the stress, failure occurs. The result is an accumulation of blocks localized along a few points of contact or in a long ribbon wandering aimlessly across the sea ice scene (Figure 5). The latter is often related to the compression of thinner and therefore weaker ice formed in a lead system between two larger floes. In any event, the accumulation is a haphazard structure of blocks piled one on top of another, some balanced in barely stable positions. The structural integrity of the upper portion of the ridge increases as initial brine drainage from the blocks refreezes and fuses the blocks together.

Additional bonding develops if surface melt occurs and refreezes. The blocks in the ridge keel will grow together if they possess sufficient heat sink capacity to freeze all or part of the sea water occupying the interblock voids.

If the momentum of the converging floes is not checked during initial impact and ridge formation, deformation continues here and there and a hummocky field is formed. Such a field is a haphazard accumulation of blocks which completely destroys the original floe scene. Hummock fields most often consist of a chaotic rubble of randomly dispersed block structures as shown in Figure 6. On occasion, hummock fields can take on a rather uniform overall appearance not unlike that of a farmer's harrowed field (Figure 7a, 7b, 7c).

If the sea is shallow the keels of ridges or hummocks may ground. Floes moving in upon such anomalies will fail as they try to climb up or push the immobile mass aside. The result is the formation of great islands or ramparts of hummocked ice as shown in Figures 8, 9, 10 and 11.

Shear ridges form as a result of extensive shearing and grinding between two ice sheets. The largest shear ridges generally occur between the moving pack and the shore-fast ice. A shear ridge may be a local phenomenon or may consist of a sinuous wall tens of miles long (Figure 12). The ice in the shear zone undergoes extensive disaggregation and consists of a highly compact granular mass. The ridge shown in Figure 12 has a near vertical face so sculptured as it scraped past higher ice anomalies along its path. This shear ridge formation is

typical of those found at the boundary between fast ice and the moving pack. Figure 13 shows a shear ridge formed near the boundary of a large floe (on the left) and a highly fragmented area (to the right).

The aforementioned deformation structures are impediments which cannot always be avoided by a ship. When these obstacles must be traversed it would be most desirable to do so by breaching their weakest section. Therefore, a better understanding of the morphology of deformed sea ice would be an important aid to the efficient and safe maneuvering of ships through arctic seas.

A preliminary field investigation of the general configuration and physical properties of pressure ridges off Point Barrow, Alaska, was undertaken by USACRREL for the U.S. Coast Guard in April 1969. The results of this investigation are presented in the report, "On Pressure Ridges" by W.F. Weeks and A. Kovacs (1970). In addition to discussing the 1969 field results, the report is a synopsis of the overall phenomenon of pressure ridging.

As a continuation of the initial reconnaissance, an investigation was planned to study in more detail the overall surface and subsurface configuration of pressure ridges. Although initially broad in scope the planned program was highly restricted due to field transportation difficulties, adverse weather and above all equipment damage in transit. This report presents the results of three cross-sectional profiles obtained in March 1970 off the U.S. Coast Guard icebreaker Northwind (WAGB 282)

during its winter cruise in the Bering and Chukchi Seas and two profiles obtained in April near Herschel Island off the arctic coast of Canada.

## STUDY AREAS

### Bering and Chuckchi Sea Profile Sites

The Bering and Chuckchi Sea profiles sites as well as the route of the Northwind between 19 February and 22 March are shown in Figure 14. Winter conditions over the area are generally bad and very changeable. Good weather is the exception. Wind shifts are both frequent and rapid but winds are usually from the north during the winter and from the south in the summer (U.S. Coast Pilot No. 9, 1964). The prevailing winds in the winter cause an overall southward ice drift from the Chuckchi Sea to the Bering Sea. However, at no time is the sea one solid sheet of ice. Local winds and currents\* are constantly changing the sea ice scene by causing areas of compaction. Up to 75% of the accompanying deformation is in the form of thrust structures (Fig. 15, 16, 17) and rarefaction which leaves 10 to 30% of the sea either open water or covered with thin (< 5 cm) ice at all times (Fig. 17, 18 and 19). Average temperatures from January through March are below -20C between 40 to 50% of the time and below -40C 1% of the time (Rayner, 1961). Undeformed sea ice generally grows to a thickness of 1.3 to 1.5 m but may reach 1.8 m in sheltered embayments or where it comprises the fast ice along the coast (Bilello and Bates, 1966 and 1969).

---

\*36% of the water entering the Arctic Basin comes through the Bering Strait (Molly, 1969).

The first ridge profile was made on 7 and 8 March while the Northwind was hove to off Port Clarence on the Seward Peninsula of Alaska. The ridge was located some 10 kilometers southwest of Lost River (Fig. 14). It (Fig. 20) had formed several days earlier under the driving force of a southerly storm.

The second two profiles were obtained on 18 and 19 March during a ten-day period in which the Northwind was nipped in the ice. The hummock field in which the ship was locked formed during a three-day storm which began on 14 March. Storm winds were from the north at 30 knots with gusts up to 50 knots. From 15 to 17 March, the ice field and icebound ships were blown approximately 23 miles south toward the Bering Strait (Fig. 14) against a northward current of 2 to 3 knots. An aerial view of the icebound ship and the surrounding hummock field on 21 March is shown in Figure 21. The first profile was made off the port side of the ship (Fig. 22 and 23) and the second profile approximately 75 m in front of the ship's bow (Fig. 23 and 24).

#### Beaufort Sea Profile Site

The Beaufort Sea study site was located approximately 7 kilometers east of the Canadian Polar Continental Shelf Project's DECA station (the old R.C.M.P. Post) on Herschel Island off the Yukon coast of Canada (Fig. 25a and b). The Herschel Island area of the Beaufort Sea is frozen over in winter with new ice averaging 1.7 to 1.9 m thick and on occasion reaching a thickness of 2.2 m. (Bilello and Bates, 1966 and 1969). Beyond the shore-fast ice, the new ice is influenced by the clockwise

circulation of the Pacific Gyral and local winds which are generally from the west or northwest. However, a wind shift of  $180^\circ$  is not uncommon. The polar pack which moves southwards off the north coast of Prince Patrick and Banks Island and then turns westward off Mackenzie Bay subjects the winter ice to enormous pressures. These forces are constantly changing the relative floe density by causing fracturing, compaction and rarefaction (Fig. 26). As a result, open water or thin ice exists in 5 to 10% of the winter sea. From January through March temperatures are below  $-20^\circ\text{C}$  80 to 90% of the time and below  $-40^\circ\text{C}$  1 to 5% of the time (Rayner, 1961).

Ice conditions east of Herschel Island on 12 April and the location of the study area are shown in Figure 27. A close-up aerial view of the ridgeline studied and the two profile locations are presented in Figure 28. The first profile was made on 9 April and the second on 10 April.

#### PROFILING TECHNIQUES

As Weeks and Kovacs (1970) state, the majority of available information on the form of pressure-related sea ice structures is based on observations of either the upper surface (visual, air photos, radar, laser altimetry) or the lower surface (sonar directed upward from below). There is no known way to simultaneously measure the upper and lower surfaces of sea ice other than by coring. However, this method does not provide a continuous profile, is extremely time consuming and fatiguing, and is nearly impossible to use beyond a depth of 15 m with manual equipment. The advantage of coring is that it does permit an examination of the subsurface structure.

The profiles presented in this report were obtained primarily by taking surface elevations using standard surveying techniques and by mapping the keel using sonar. Additional profile data were obtained by coring.

The sonar transducer used had a 7° beam width between the 3-db points. The transducer was fixed to the end of an aluminum rod extension system which enabled the transducer to be lowered beneath the ice and pointed in any desired horizontal direction. To profile the keel of a ridge, the transducer was lowered below the thinner ice adjacent to the ridge. With the transducer pointed at the keel, the horizontal distance between the transducer and the keel was measured acoustically. By repeating this measurement at many elevations the contour of the keel was determined. An indication of the type of recordings obtained is presented in Figure 29. This particular record shows the measurements obtained at Profile 2B when the transducer was lowered the first 38 ft (~ 11.5 m) below the ice surface.

#### PROFILES

An aerial view of the first ridge studied (Fig. 20) shows that it consisted of an assortment of blocks of various sizes and that a relatively large crack divided the ridge. The largest blocks were 1.6 m thick, comparable to the thickest plate ice in the area. Much thinner ice was also found incorporated within the ridge (see Fig. 30 of the north face), indicating that floes of different thicknesses

had participated in the formation of the ridge. Many of the blocks were found in barely stable positions. Caution had to be exercised when walking as these blocks would often slip out from beneath the feet. Blocks weighing several hundred pounds were unintentionally dislodged this way and could be dislodged intentionally with a strong kick. The reason for the poor bonding between the blocks in the upper part of this ridge, is related to insignificant interblock bond growth at the low temperatures (-20 to -40C) existing during the short life of the ridge.

The crack appeared to be related to a slight southerly drift of the pack shortly after the ridge formed. Access into the crack cavity was possible by climbing down through the block canopy. The floor of the crack (approximately 1 m wide) consisted of newly forming sea ice. This surface was probed with a meter stick and found to be 4 cm thick. Below this was a layer of water followed by a second layer of ice not as thick as the first. A third layer of ice was similarly found. This indicates that the ridge had undergone isostatic adjustment with each layer representing a migration of the sea upward as the ridge subsided.

The fact that the ridge was undergoing isostatic adjustment was also apparent along the entire south edge. Here successive layers of refrozen sea water could be seen covering the ice adjoining the ridge. Each represented an upward flow of water as the adjoining plate ice was deflected beneath sea level by the weight of the subsiding ridge. A view of the south face is shown in Figure 31.

The cross-sectional profile of the ridge is presented in Figure 32. The line along which the profile was made is shown in Figure 20. The highest elevation on the profile is 7.1 m at station 50 M. While the lowest point of the ridge could not be determined because of sea floor interference with the reflected transducer signal, the shape of the subsurface profile indicates that the ridge is grounded in 13.7 m of water.

Twelve holes were augered to determine ice thickness along the profile line. Cavities were found at the four stations shown in Figure 32. In general the ice became softer with depth as determined by drilling ease.

The direct and sonar measurements of the bottom contour of the north side of the ridge apparently disagree. This is not surprising, considering the size of the area investigated with each technique. When augering to determine ice thickness, the procedure was to drill until the apparent bottom was reached. At this point the auger was lowered an additional  $1\frac{1}{2}$  m. If no further ice was encountered, it was assumed that the bottom of the keel had been penetrated. The size of the area penetrated is, of course, related to the thickness of the auger (4 cm). It is possible that the auger may have entered an opening, between the block structure, leading to the underside of the keel at station 80 M. However, because of the large difference between the drill hole measurement and the sonar measurement at

station 75 M, it can be postulated that the auger was not lowered far enough to insure that the bottom of the keel had indeed been penetrated.

While the drill hole measurement provides ice thickness at a point, the sonar because of its beam angle measures a larger and therefore multi-distant surface. A discriminating interpretation of the sonar record allows one to construct a profile much more representative of the overall keel contour than is possible by drill hole measurement. For this reason, sonar profiling is preferable.

The slope of the surface and subsurface faces varies from a low of ~~The angle varies from a low of approximately 20° to a high~~ approximately 20° to a high of 55°.

~~xxxxxx~~ The above-surface angles average 24°. This is in the 20° to 30° range suggested by Zubov (1945). Similarly the average subsurface slope angle is approximately 38°, or 6° greater than the average value determined by Wittmann and Schule (1966) from submarine sonar profiles of 39 ridges.

Profile 2A was made of the port side of the Northwind (see location on Fig. 23) to determine the depth of ice underneath the ship after it became nipped. The size of the ice blocks and the roughness of the terrain alongside the icebound ship are clearly shown in Figures 33 and 34. The arrow in Figure 22 points to the augered hole through which the sonar transducer was lowered. The hole was 9.0 m in depth. Two cavities were encountered as shown in Figure 35. The first was  $\frac{1}{2}$  m thick and the second  $1\frac{1}{2}$  m thick. Other than these two cavities the ice was found to be "firm" over the entire depth. From the sonar trace it was evident that this hole had been augered through the thinnest ice in the area. The sonar profile (Fig. 35) shows that the ice increased in thickness

both toward and away from the ship. This was also found to be the case when the sonar transducer was pointed in the forward and aft direction.

The sonar profile in Figure 35 shows that the ice to the left of the augered hole reached a depth of approximately 14 m below sea level or 6 m lower than the keel of the ship. Unfortunately, the profile extending under the ship is incomplete. Loss of lowering rods limited to 18 m the depth to which the transducers could be lowered below the ice surface.

A partial cross-section profile was obtained of the hummock field (Fig. 24) in front of the Northwind. This profile (Profile 2B) is presented in Figure 36 and its location in relation to the Northwind is shown in Figure 23. The sonar measurements were terminated at a depth of 19 m for lack of additional lowering rods as previously discussed.

Initially it was planned to take sonar measurements from station 25 M, the assumption being that the keel of the hummock field began under the surface near station 24 M. After several meters of ice had been augered it became apparent that this was not the case. Drilling was then continued in hopes of measuring the thickness of the ice at this station. However, ugering was stopped at the 11-m depth due to mechanical difficulties. Down to this depth the ice was surprisingly voidless and firm. Sonar measurements were made from station 9 M.

Disregarding the anomalous protrusion around the 17-m depth, the slope angle of the keel (Fig. 36) is approximately  $35^{\circ}$ .

Measurements in reference to this angle revealed that the ratio of the elevation of the ice above sea level to that below averaged 1 to 7 between stations 10 M and 25 M. The ratio increased to 1 to 16 at station 30 M and 1 to 19 at station 35 M.

The average slope angle of the south-facing blocks in the three central humps on the surface profile is approximately  $15^\circ$ . The same angle for the north faces is approximately  $30^\circ$ . The overall average is 25 .

Profile 3 (Fig. 37) was taken over a high section of a large ridge system (Fig. 28) which formed off the eastern tip of Herschel Island. A ground view of the ridge is shown at the rear center of Figure 38. The path shown leading up the face of the ridge marks the line along which the profile was made.

The highest point on the profile is at station 82 M where the ridge reached a height of 11.4 m above sea level. The highest point on the ridge was several meters north of the profile line (Fig. 38). Here the ridge was 2.1 m higher or 13.5 m (~ 44 ft) above sea level.

Snow covered much of the ridge. Along the edge of the ridge drift snow reached depths in excess of 4 m. Probing along the base of the ridge revealed the existence of slush underneath the snow cover, an indication of salt water intrusion. Also noted were a number of tension cracks in the snow crust along the base of the ridge. This observation and the fact that the ice surface has been deflected downward

at the base of the ridge (Fig. 37) suggest that the ridge is subsiding and, in the process of load transfer, has caused the surrounding ice to deflect downward.

The slope angle of the blocks on the west face of the ridge is  $22^\circ$ . The angle on the east face is  $22^\circ$  as drawn on Figure 37 and it is approximately  $27^\circ$  on the outer steeper face.

An exploratory hole at station 30 M revealed the following: 0 to 6 m hard ice, 6.0 to 7.2 m void, 7.2 to 8.2 m soft ice (believed to be ice formed in a cavity) 8.2 to 9.3 m void, 9.3 to 10.2 m soft deteriorated ice, and 10.2 to 11.2 m firm ice. Coring was halted at 11.2 m (35.5 ft).

Sonar measurements were taken of the keel on the west side of the ridge (Fig. 37). These revealed that the ridge was grounded in only 13.3 m (43.5 ft) of water.

The ratio of the elevation of the ice surface above sea level to the depth below is 1 to 10 at station 4 M, 1 to 17 at stations 8 and 12 M, 1 to 19 at station 16 M, 1 to 17 at station 20 M and 1 to 13 at station 24 M. These large ratios are far above the 1 to 7 isostatic ratio normal for free-floating sea ice. The implication here is that the keel is highly porous and therefore less buoyant. Indeed large voids were encountered in the exploratory hole along with zones of deteriorated (porous) ice. However, load transfer from the ridge proper is undoubtedly significant and therefore responsible for the low surface elevation.

Profile 4 was located a short distance from Profile 3 as shown in Figure 28. A ground view of the block structure in the ridge is shown in Figure 38. The ridge cross section is presented in Figure 39. Here it is seen that the slope angle of the surface structure is not well defined. An angle of  $15^\circ$  is shown only for general reference. The slope angles of the keel are well defined and are  $48^\circ$  for the south face and  $34^\circ$  for the north.

The ice on the south side of the ridge was found to be just under 2 m thick while on the north side it was over 5 m thick. Coring on the north side revealed two layers of ice separated by a cavity up to 1.3 m thick. The lateral extent of the cavity in the profile plane at station 59 M was found by sonar measurement to be 2.5 m wide (Fig. 39). The layering is a result of rafting during which the two sheets were separated by fragments of ice presumably broken off their leading edges. The direction taken by the overriding sheet is shown by the lower arrow in Figure 28. As would be expected, when two ice sheets move tangentially to one another, shearing will occur. Figure 28 clearly shows that this did occur. In short, Profile 4 is a unique example of rafting in ice approximately 2 m thick.

#### DISCUSSION

The density of sea ice depends upon its salinity and in particular upon its porosity. In plate ice, i.e. undeformed sea ice, the density

often ranges between 0.87 and 0.94 g/cm<sup>3</sup> or averages about 0.91 g/cm<sup>3</sup>. The depth at which an ice floe floats varies with its density ( $\gamma_1$ ) and the density of the surrounding sea water ( $\gamma_w$ ) which often is 1.03 g/cm<sup>3</sup>. In this environment an ice floe having an average density of 0.91 g/cm<sup>3</sup> will have a 1 to 7.6 ratio between its above-water height ( $h_1$ ) and submerged portion ( $h_2$ ). This ratio is based on Archimedes' principle of buoyancy where:

$$\frac{h_1}{h_2} = \frac{\gamma_w - \gamma_1}{\gamma_1}$$

Likewise, an ice floe with an average density of 0.90 g/cm<sup>3</sup> will have a ratio of 1 to 7.0. The open block structure of a hummock field on the other hand may have an average density of 0.75 g/cm<sup>3</sup> and therefore a ratio of only 1 to 2.7 between its above-water and submerged portions. These ratios, of course, are based upon the assumption that the ice is isostatically compensated.

The  $h_1/h_2$  ratios reported here are for the most part higher than 1 to 7. Thus, the ice where the measurements were made was not in isostatic equilibrium. It is assumed that the ice was being deflected downward by load transfer from higher portions of the surrounding ridge. A similar finding was made by Weeks and Kovacs (1970).

From the highest point above sea level to the lowest point below, on Profile 4, the  $h_1$  to  $h_2$  ratio is 1 to 4.5. If the abrupt horizontal

shift in the subsurface contour of Profile 2A (Fig. 36) indicates that the bottom of the keel was nearly reached, and it is assumed that the bottom is 0.5 m below the last sonar measurement, then the  $h_1$  to  $h_2$  ratio for the first rise on the surface profile is approximately 1 to 5. Similar ratios for Ridge A2a, b and c, Ridge A3 and Ridge A7 studied by Weeks and Kovacs are 1 to 4.5, 1 to 9, 1 to 3.5, 1 to 3 and 1 to 4.6 respectively. Combining these ratios with the two above, the average  $h_1$  to  $h_2$  ratio is 1 to 4.9. If the anomalous 1 to 9 ratio for Ridge A2b is not included, the average ratio becomes 1 to 4.2. In short it appears that a rough estimate of the maximum depth of a ridge keel can be determined by multiplying its height above sea level by a factor of 4 or 5.

Slope angles presented on the pressure structures studied in this paper averaged  $24^\circ$  for the surface faces and  $36^\circ$  for the subsurface faces. Slope angles of the structures studied by Weeks and Kovacs (1970) averaged  $25^\circ$  (surface) and  $32^\circ$  (subsurface) and by Wittmann and Schule (1966)  $32^\circ$  (subsurface). Although the surface or subsurface slope angles can vary from  $10$  to  $60^\circ$  at any one ridge, the angles listed above indicate that the subsurface angle of repose averages 5 to  $10^\circ$  greater than the surface angle.

As Weeks and Kovacs (1970) state, "Several different 'models' have been proposed for the overall shapes of pressure ridges." Burke's (1940) suggestions are that the edges of the above-and below-block structure of a ridge start at similar locations, the

slope of the above-surface face is equal to or less than that of the submerged face and the plate ice on either side of the ridge is deflected downward by the weight of the ridge. The Wittmann and Schule model shows a gradual increase in the elevation of the ice surface approaching the ridge and then an abrupt increase in the slope at the ridge proper which is much greater than the slope of the keel. Their model shows that the edge of the keel starts where the surface begins its gradual increase in elevation rather than at the location of the abrupt slope increase at the ridge proper. The Burke model agreed with the ridge studies made by Weeks and Kovacs and with the findings shown in this report for the south side of Profile 1 as well as the north side of Profile 4. For the other side of these profiles and the other profiles presented here, a modified Wittmann - Schule model would be more representative. The modified model would show the upper slope of the ridge proper to be less than that of the keel. It should be pointed out that neither model was intended to represent the structural configuration of a hummock field.

One of the earliest studies of the formation and structure of pressure-related sea ice structures is that by Archowski (1908). His observations were made during the cruise of the S.Y. Belgica (1897-1899) in the Antarctic pack. His findings on one ridge are as follows: (1) The symmetry is imperfect; (2) there is a relatively thin ice field in contact with another of thicker ice and it is the thinner ice, pushed against the thicker, which was unable to resist

the pressure and fragmented; (3) ahead of the ridge there is a strong inflection of the ice covered with snow and thereby leveled, but the ice rises towards the summit; (4) there are a number of open cavities, indicating a block structure, and the submerged protuberance is not very firm, and (5) there are loose fragments of ice near the submerged keel of the ridge. Archowski's interpretations related to this ridge are similar to recent observations made by Weeks and Kovacs (1970) during their study of ridging at Barrow, Alaska, and to the observations presented here. In addition Archowski's sketches of ridge configuration include the model shape proposed by Burke (1940) and that of Wittmann and Schule (1966). Archowski was perhaps the first to describe the keel of a ridge as a honeycombed structure resembling a huge sponge with irregular contours and to determine that sea ice movement and deformation occurs primarily as a result of wind stress. He also described events leading to rapid and slow ridge formation and events leading to the complete destruction of the original ice canopy. In short, Archowski was an astute observer of the cause and effect of sea ice movement, fracture and deformation, and although his work is little known today his studies do remove much of the confusion from an otherwise chaotic scene.

On the 1969 voyage of the S.S. Manhattan through the Northwest Passage, it was noted that new pressure ridges did not offer significant resistance and could be penetrated without difficulty (Weeks and Kovacs, 1970). This was because the ice blocks in new ridges

are not well bonded together. Old ridges (more than one season old) however did create significant resistance to penetration. Such ridges were found to be voidless. Presumably the interblock voids were filled with refrozen summer melt which greatly increased the structural integrity of the ridge which in turn reinforced the surrounding floe ice.

Observations made during the 1970 winter cruise of the Northwind showed that it could penetrate (without ramming) pressure ridges up to 2 m high when the surrounding ice was in a state of rarefaction and the ridge was not "wide" (Fig. 40). It was found that even under rarefied conditions a wide ridge was difficult to penetrate. This was not only due to the resistance of the ridge itself but more so to the energy-absorbing capacity of the broken-up ridge debris in the ship's channel. At times this debris would completely cushion the ship's forward motion, preventing it from attacking the ridge. This is illustrated in Figures 41, 42 and 43. Figure 41 shows the rarefied ice environment the Northwind was penetrating on 13 March in the area of the Arctic Circle. The closeup aerial view of the same scene (Figure 42) shows the ship backed off from a ridge it could not penetrate after repeating<sup>ed</sup> ramming. The thick accumulation of broken ice in the channel near the ridge reduced the ship's ramming speed to the point of ineffectiveness. A closeup view of the ridge and the ice-clogged channel is shown in Figure 43.

It was also observed that rafted areas offered appreciably greater resistance to penetration than ridges of considerably greater thickness. The most difficult rafted areas to negotiate were those with large accumulations of blocks at the leading edges of the thrusts. The resistance of the doubled ice thickness and the energy adsorbing capacity of the block structure debris in the channel were the cause of much ramming and, of course, delay.

While a detailed discussion on the decay of pressure-related sea ice structures has been given by Weeks and Kovacs (1970), a short summary of the metamorphic process as described by Thoren (1969) should be of interest:

"Ice is evaporated and melted by direct absorption of sun radiation and by conduction of heat from the surrounding air and water. The albedo or the percentage of incident light reflected from a surface is about 50% from sea ice but only 3 or 4% from sea water. As regards to the infrared portion of the spectrum, representing heat energy, the proportions reflected by ice are about 12% and by water 1%. Further, as water is opaque to infrared radiation, the heat adsorption by water is concentrated in the uppermost layers where the ice is floating. An ice-covered surface with leads and other water openings or pools of meltwater accumulating on top - so called puddles - therefore will absorb considerably more radiant heat than a continuous ice surface. Thus, as soon as free water surfaces appear, the rate of further disintegration is accelerated. A lowering of the albedo of the ice, for instance through the accumulation of dust [or plankton, see Fig. 44] will also speed up disintegration.

Melting takes place as soon as the temperature of any superficial layer of the ice is raised above the freezing point. Evaporation, on the other hand, may occur at any temperature. Young ice melts more readily than older ice because of its higher salt content. Having a structure of nearly salt-free ice and a minimum of exposed surface in proportion to their bulk, hummocks of old Arctic pack will resist melting the longest."

#### CONCLUSION

This report presents additional information on the configuration of pressure-related sea ice structures. It has been determined that the depth of the below-water portion of a ridge appears to be approximately 4 to 5 times the above-water height.

It was pointed out that the shape of pressure ridges was found to agree with sketches by Archowski (1908); and that the models proposed by Burke (1940) and Wittmann and Schule (1966) were found to be representative of only certain ridge configurations. Indeed there is no reason to believe that a single model can represent the imperfect symmetry of ridges formed under such variable conditions.

Although ridge sail and keel angles of repose were found to vary from 10 to 60°, the surface angle averaged 24° while the subsurface angle averaged 33°. It may be concluded that the subsurface angle of repose will be 5 to 10° greater than the surface angle.

The technique of sonar profiling was found to be an expedient method of determining the subsurface contour of a ridge. Coring through ridges was limited in this study because of equipment losses. However, coring is also recommended because it allows the determination of the internal state of the ridge.

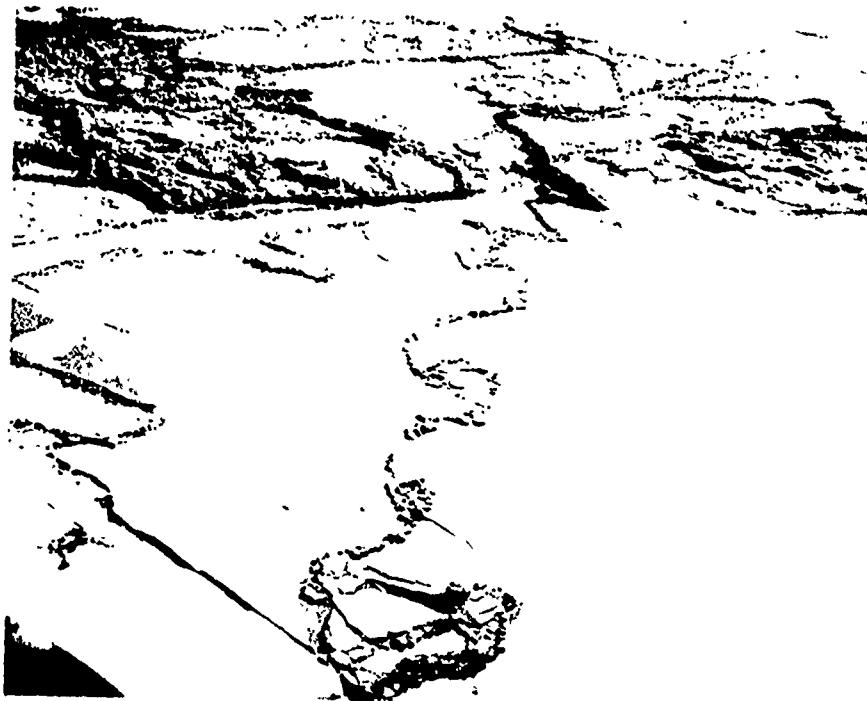
#### REFERENCES

- Anderson, V.H. and Marljar, T.L. (1969) Sea Ice Pressure Ridge Study: an airphoto analysis. USACRREL Contract Report to the U.S. Coast Guard.
- Arctowski, H. (1908) Ice - Sea Ice and Pack Ice, In Findings of the voyage of the S.Y. Belgica in 1887-1899: Scientific Reports, Vol. 5 (In French).
- Bilello, M.A. and Bates, R.E. (1966 and 1969) Ice Thickness Observations, North America Arctic and Subarctic, USACRREL Special Report 43, Pt. III and IV.
- Burke, A. (1940) Morskie l'dy (Sea Ice), Izdatel'stvo Glavsevmorputi, Leningrad. (Translation of Polar Works Library, Dartmouth College).
- Molly, A.E. (1969) The Arctic Ocean, Oceans, Vol. 1, No. 2.
- Rayner, J.N. (1961) Atlas of Surface Temperature Frequencies for North America and Greenland, Arctic Meteorology Research Group, McGill University.

- Sater, J.E. (1963) The Arctic Basin, Arctic Institute of North America.
- Thoren, R. (1969) Picture Atlas of the Arctic, Elsevier Publishing Co.
- U.S. Coast Pilot No. 9 (1964) Pacific and Arctic Coasts, U.S. Dept. of Commerce, Coast and Geodetic Survey.
- Volkov, N.A. and Voronov, P.S. (1967) Investigation of Sea Ice Cryotechnique for Glaciological and Geological Purposes. In Problems of the Arctic and Antarctic, Vol. 27 (In Russian).
- Weeks, W.F. and Anderson, D.L. (1958) Sea Ice Thrust Structures, Journal of Glaciology, Vol. 3.
- Weeks, W.F. and Kovacs, A. (1970) On Pressure Ridges, USACRREL Contract Report to the U.S. Coast Guard (In Review).
- Wittmann, W.I. and Schule, J.J. (1966) Comments on the Moss Budget of Arctic Pack Ice. In Proceedings Symposium on the Arctic Heat Budget and Atmospheric Circulation, the RAND Corp. (RM-5233-NSF).
- Zubov, N.N. (1945) L'dy Arktiki (Arctic Ice), Izdatelestvo Glavsevmorputi, Moscow.
- Zukriegal, J. (1935) Cryologia Maris (Study of Sea Ice), Geographica Institute Charles IV, Praha.



Figure 1. Finger rafting in thin sea ice.



a.



b.

Figure 2. Rafting of sea ice in excess of one meter thick. Note the extent of fracture in the thrusts and the surrounding plate ice in Figure 2a.

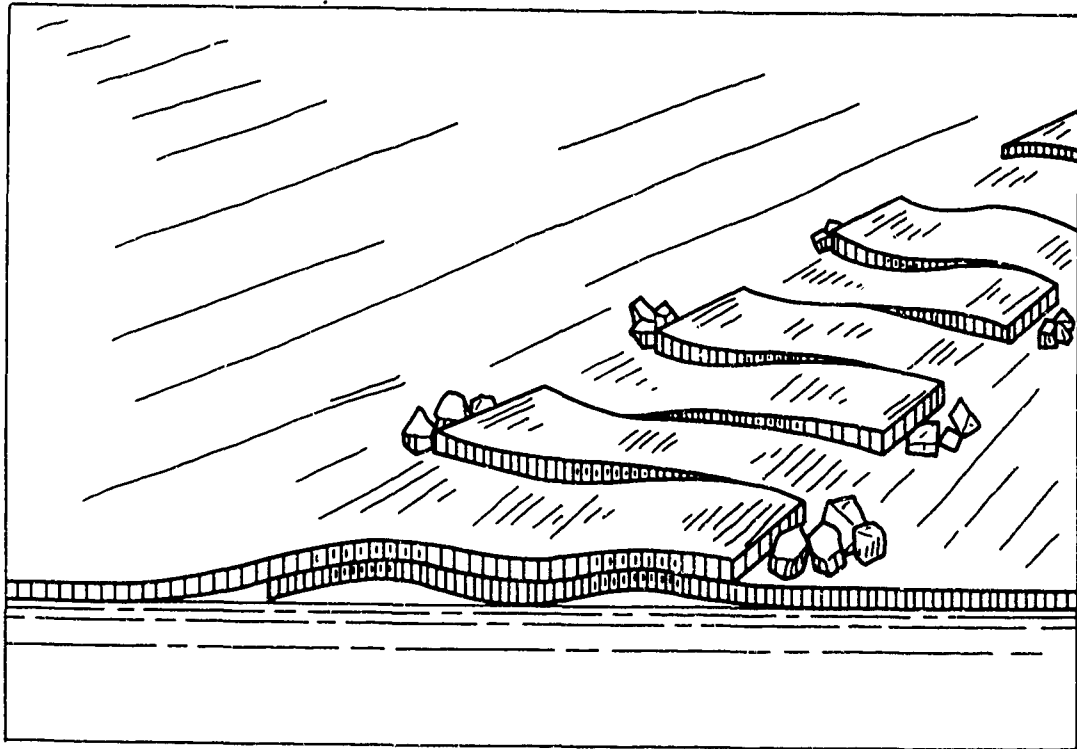


Figure 3. Sketch of finger rafting in which both participating sheets have sheared and interlocked (from Volkov, 1967).

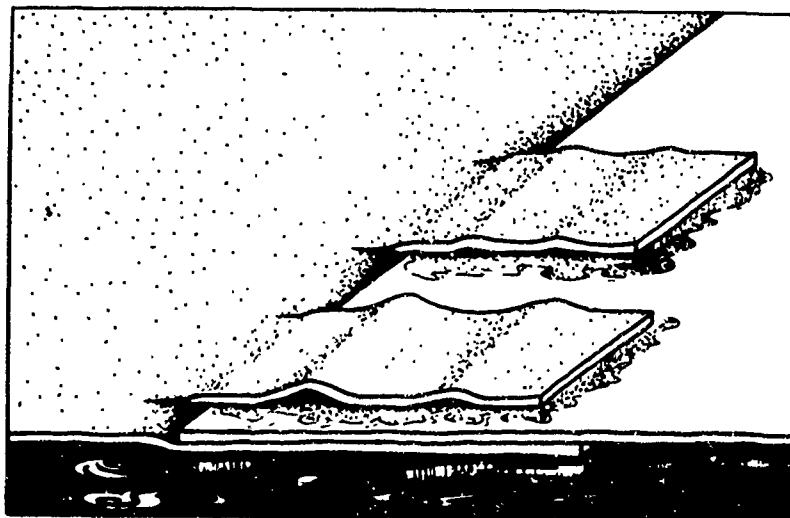


Figure 4. Sketch of rafting in which only one participating sheet has sheared (from Weeks and Anderson, 1960).  
1958

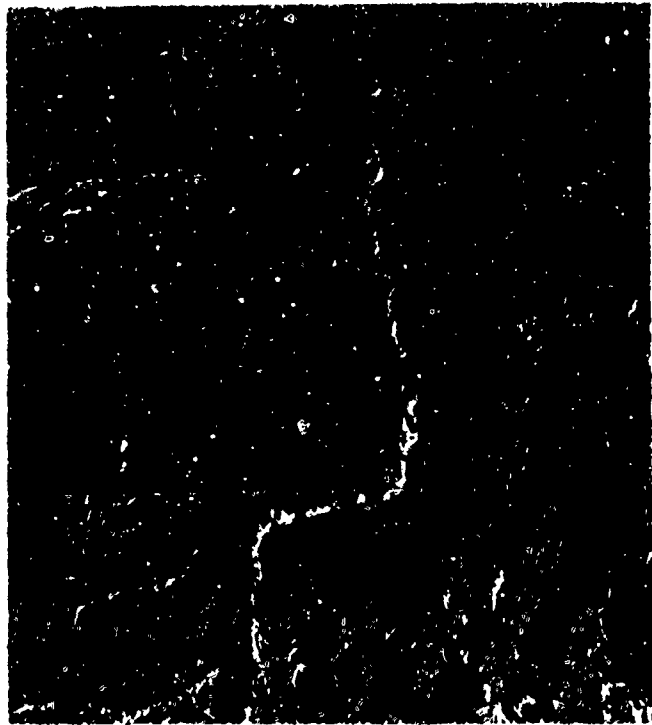


Figure 5. Long sinuous ridge observed in the Polar Pack.

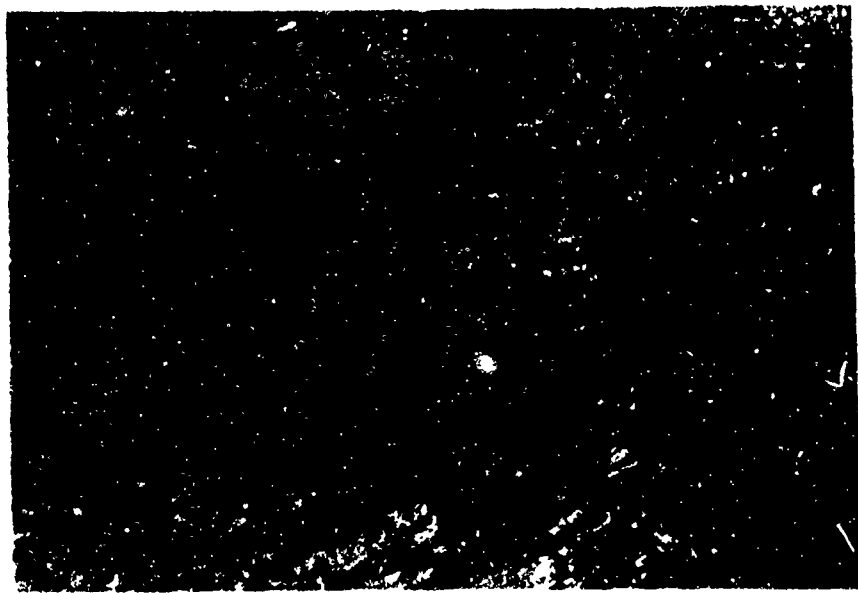


Figure 6. Extensive hummocking in sea ice east of Pt. Barrow, Alaska.

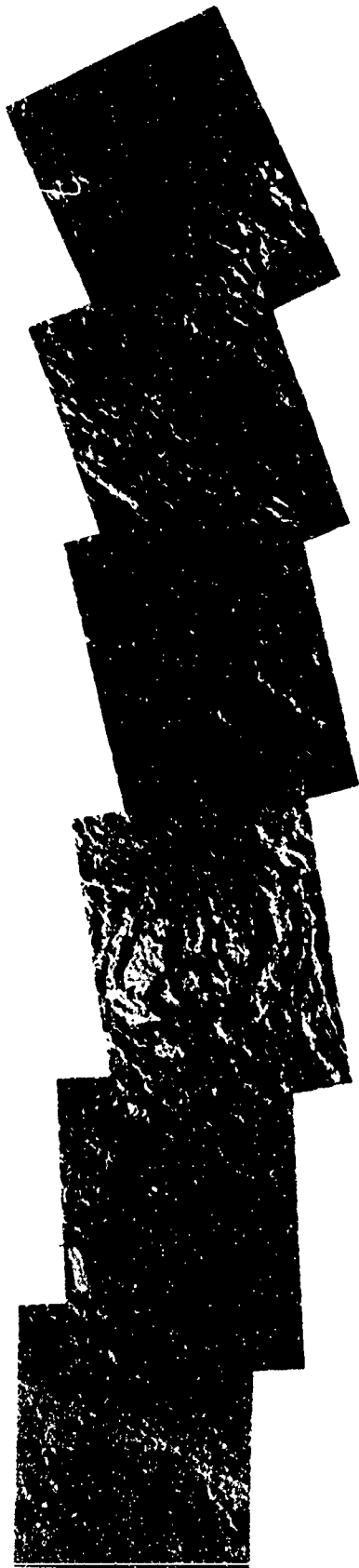


a.



b.

Figure 7. View of a rectangular hummock field observed at the Arctic Circle in the Chukchi Sea north of the Bering Strait. The ridges in the field reached heights of up to 7 m.



c.

Figure 7 (Cont'd). View of a rectangular hummock field observed at the Arctic Circle in the Chukchi Sea north of the Bering Strait. The ridges in the field reached heights of up to 7 m.



Figure 8. Large rampart of grounded sea ice west of Prince of Wales Shoal, Alaska (see Fig. 14).

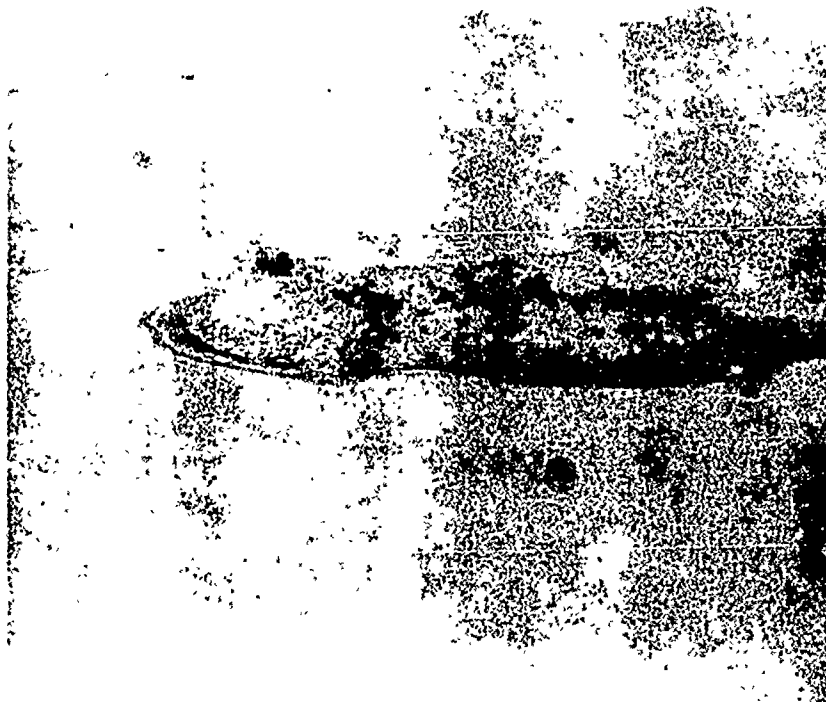


Figure 9. Large rampart of grounded sea ice west of Prince of Wales Shoal, Alaska. Note the lagoon around the periphery of the rampart. This signifies that the structure has subsided, causing the surrounding plate ice to be deflected below sea level.



Figure 10. Ground view of ice rampart shown in Figure 9. This face is approximately 14 meters high.



Figure 11. Large cross-shaped island of grounded ice east of Herschel Island, Canada (see Fig. 25). The highest point on this formation was estimated from the ground to be 17 meters high.

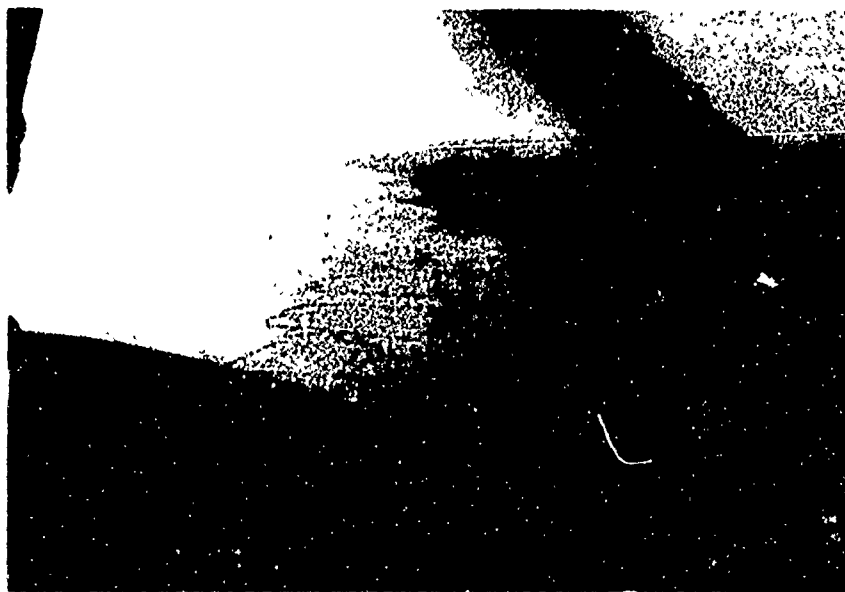


Figure 12. Shear ridge formation along the fast ice / pack ice boundary northeast of Barrow, Alaska.



Figure 13. Shear ridge formation near the boundary of a large floe and fractured ice in the Bering Sea.

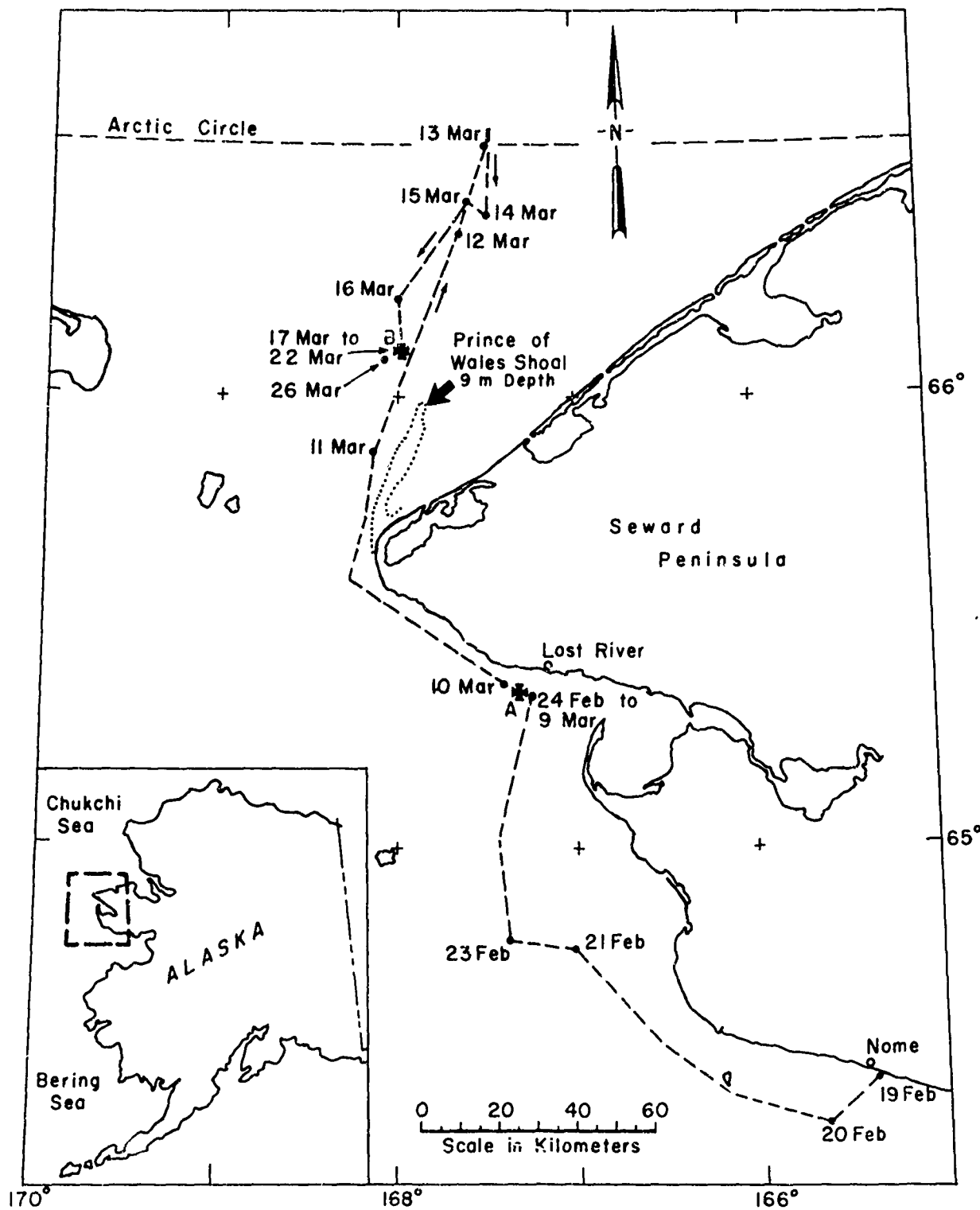


Figure 14. Location of the Bering (A) and Chukchi Sea (B) profile sites. The dashed line represents the route of the Northwind and the dots give the noon position on the accompanying date.

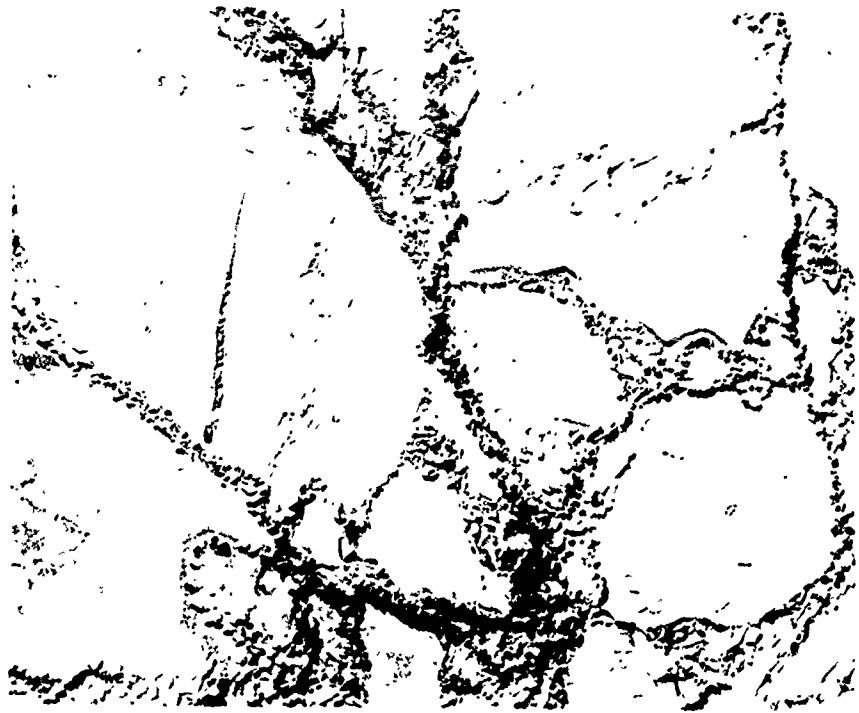


Figure 15. Raft formations in the Bering Sea.



Figure 16. Raft formation in the Chuckchi Sea north of the Bering Strait in the area of the Arctic Circle.



Figure 17. Rafting and rippling in thin sea ice, Chuckchi Sea.



Figure 18. Rarefied ice conditions in the Chuckchi Sea near the Arctic Circle on 13 March 1970.



Figure 19. Rarefied ice conditions north of the Bering Strait at the Arctic Circle on 13 March 1970.

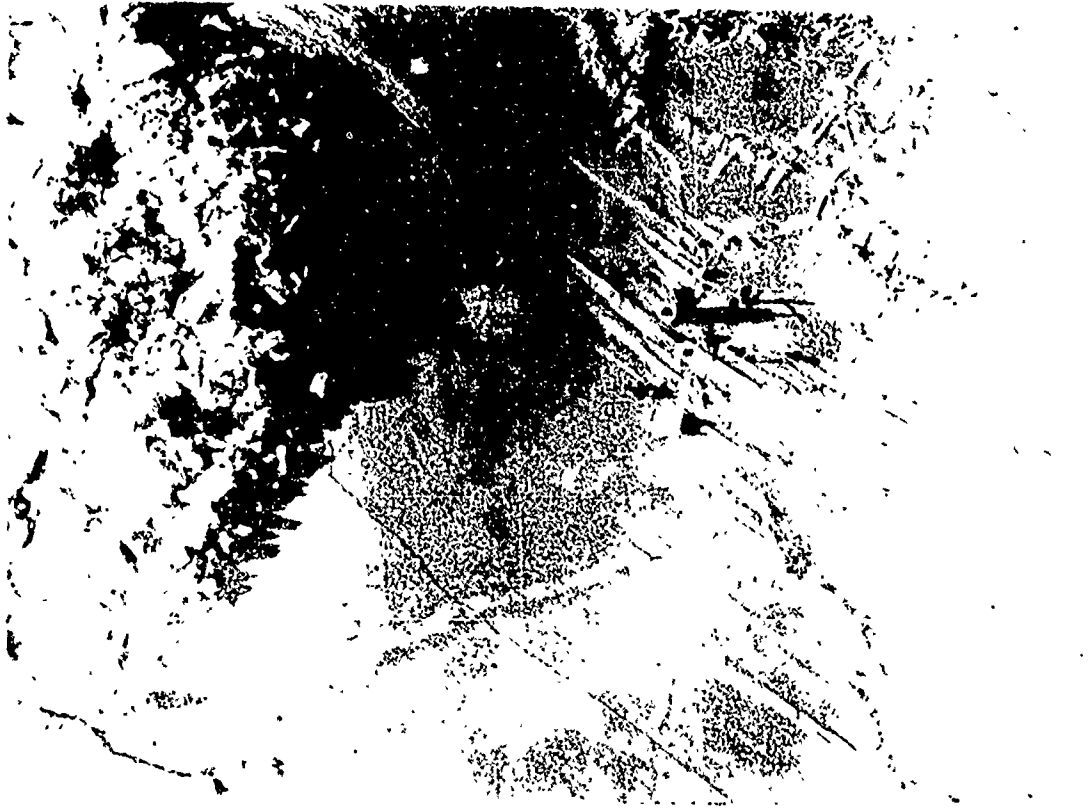


Figure 20. Aerial view of ridge studied southwest of Lost River, Alaska.  
The position of the profile line is indicated by the arrows.



Figure 21. Aerial view of the beset Northwind and the surrounding sea ice scene on  
21 March 1970.



Figure 22. Ice conditions along the port side of the be-  
set Northwind. The arrow points to the augered hole through  
which sonar profiling of the ice under the ship's hull was  
undertaken.

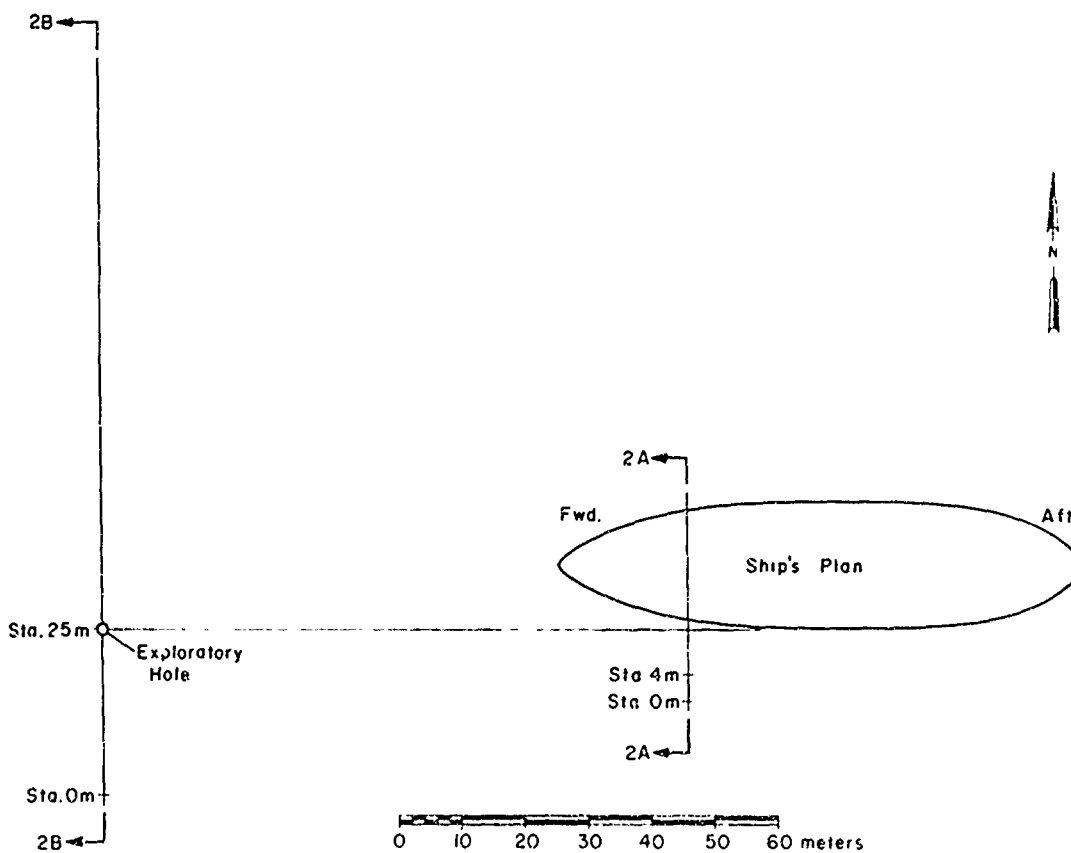


Figure 23. Plan view of Northwind and the location of Profiles A and B.

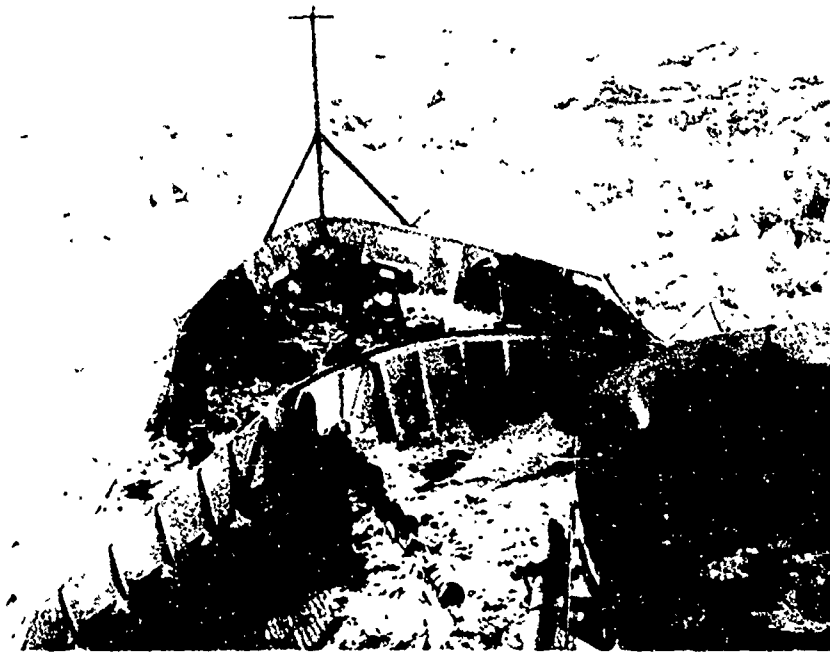
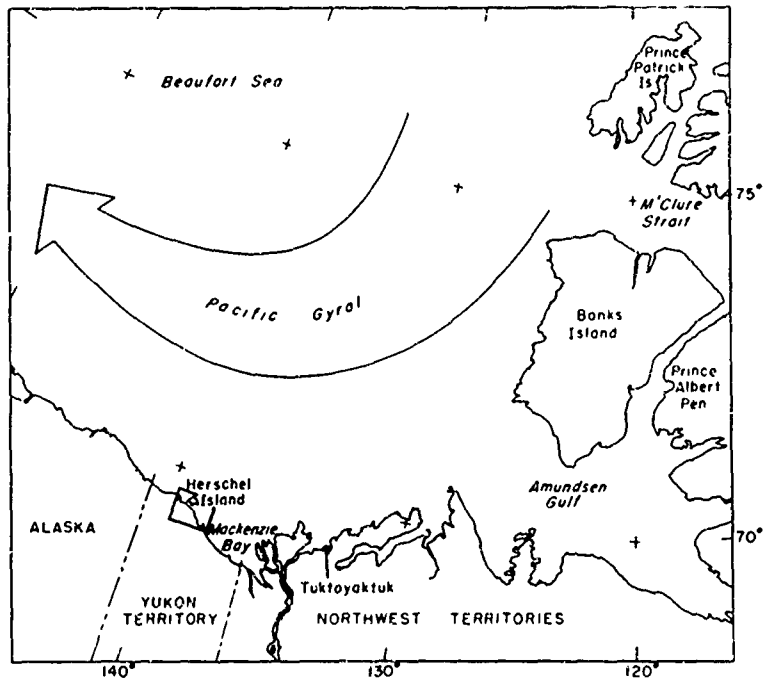
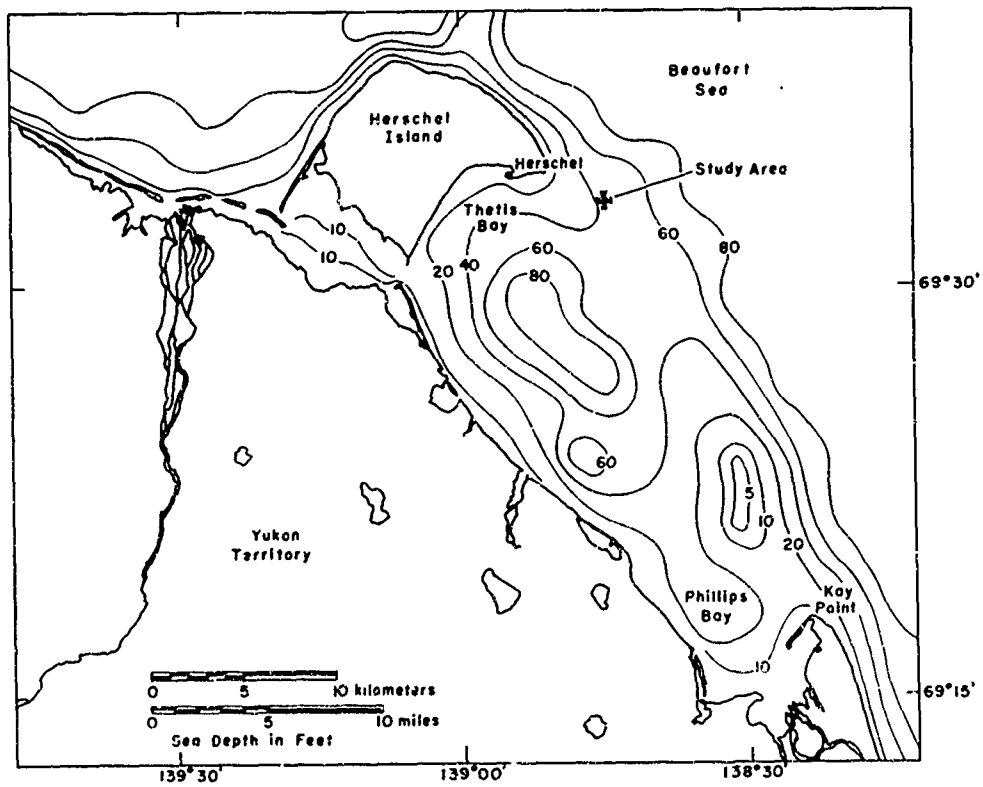


Figure 24. Ice conditions off the bow of the beset North-  
wind on 19 March 1970.



a.



b.

Figure 25. General location map (a) and area view of the Herschel Island study site (b).

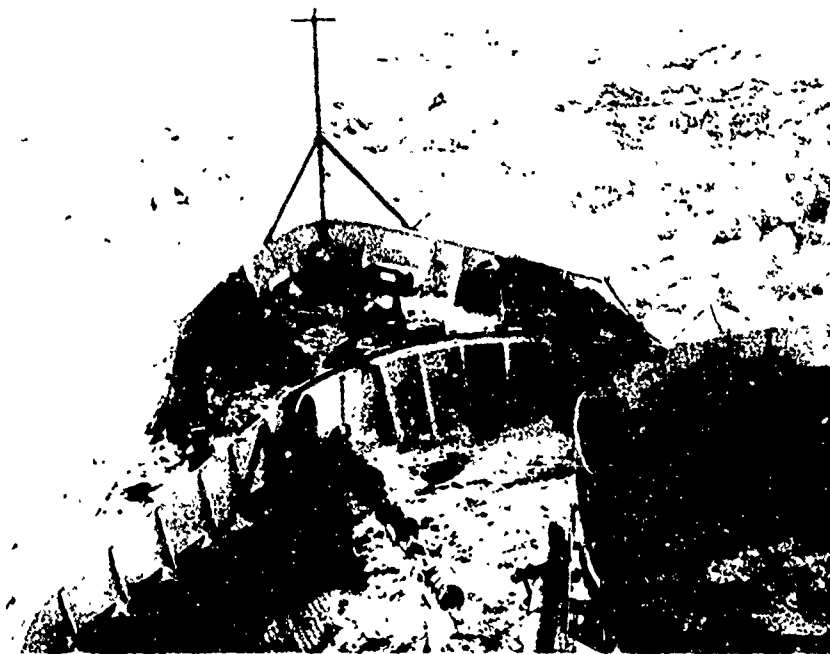


Figure 24. Ice conditions off the bow of the beset North-  
wind on 19 March 1970.

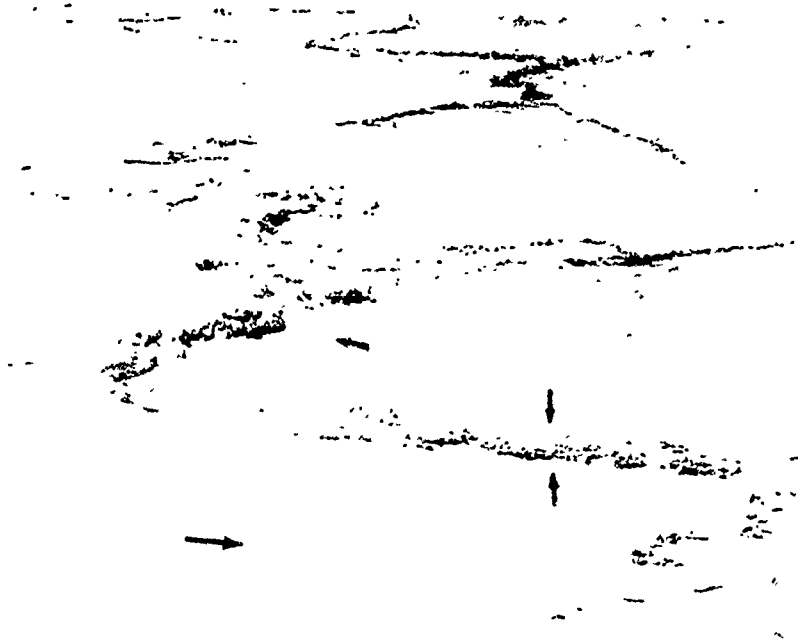


Figure 28. Aerial view of ridge line studied off Herschel Island. The upper arrow points in the general direction of Profile 3 and the two opposing arrows point out the location of Profile 4. The lower arrow indicates the direction taken by the incoming ice against the fast ice surrounding Herschel Island.

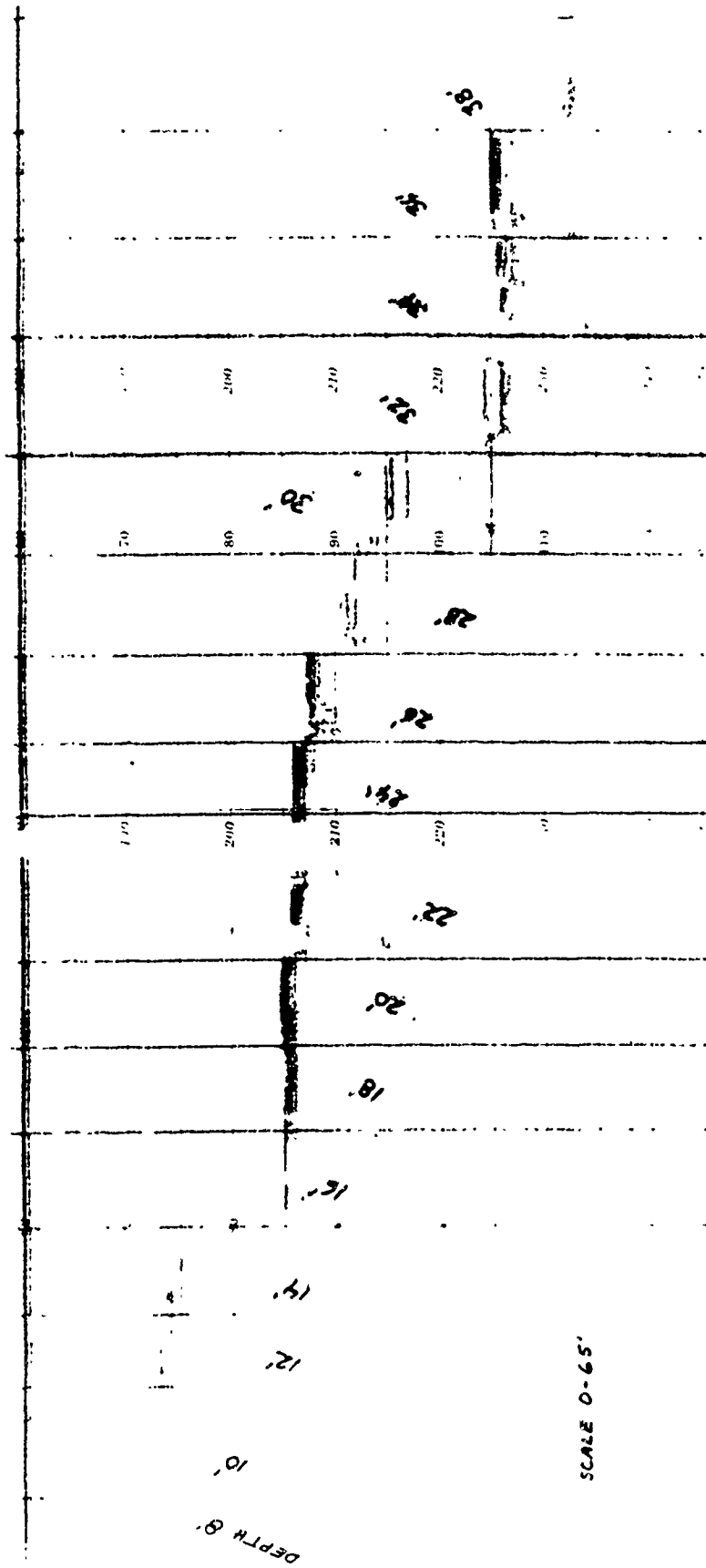


Figure 29. Sonar record obtained during contour measurement of the upper keel portion of Profile 2B.



Figure 30. North face of Profile 1 ridge showing variation in thickness of incorporated ice blocks.



Figure 31. South face of Profile 1 ridge. The man on the left is walking on an area recently flooded and refrozen. The frozen lip of this inflow is clearly visible.

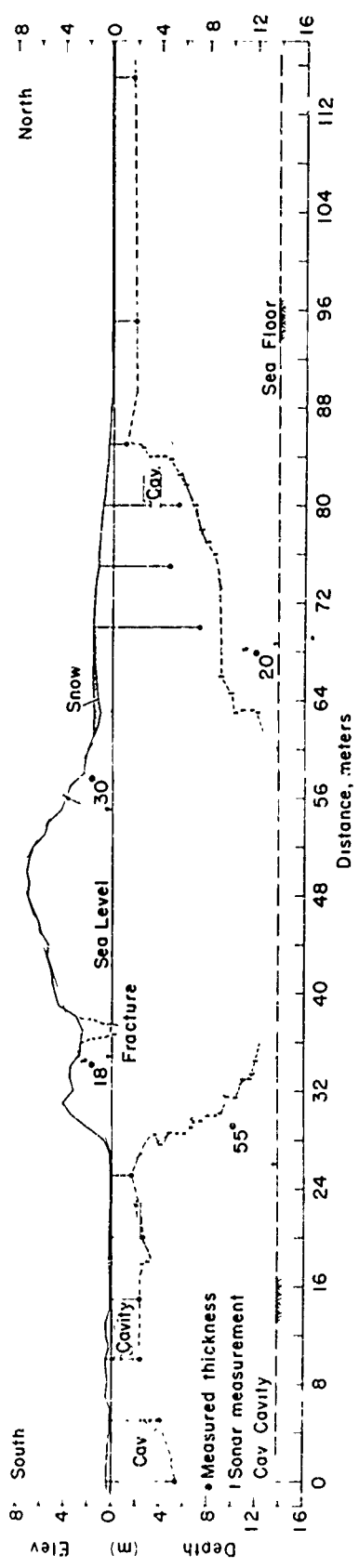


Figure 32. Profile 1. Sonar measurements were made from station 15 M.



Figure 33. Ice conditions off the port side of the beset Northwind on 19 March 1970.



Figure 34. Structure of ice block terrain in front of the Northwind on 19 March 1970. Photo was taken near station 25 M as shown on Figure 23.

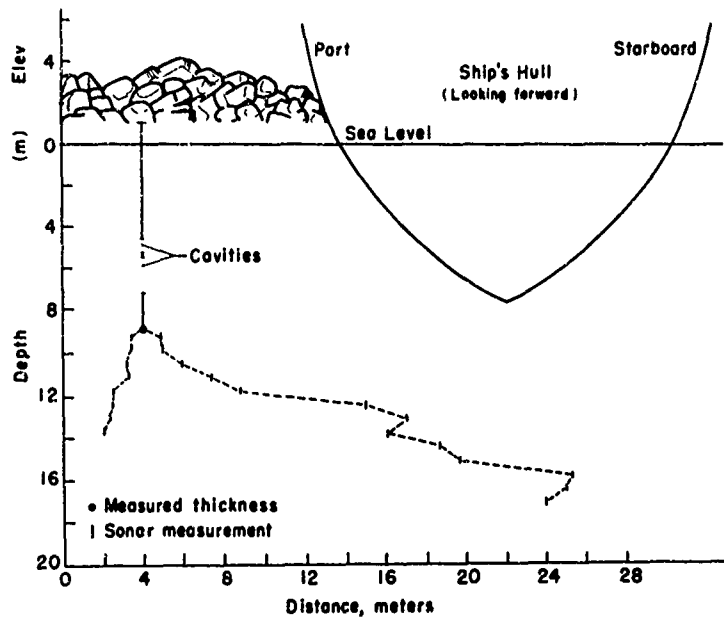


Figure 35. Profile 2A.

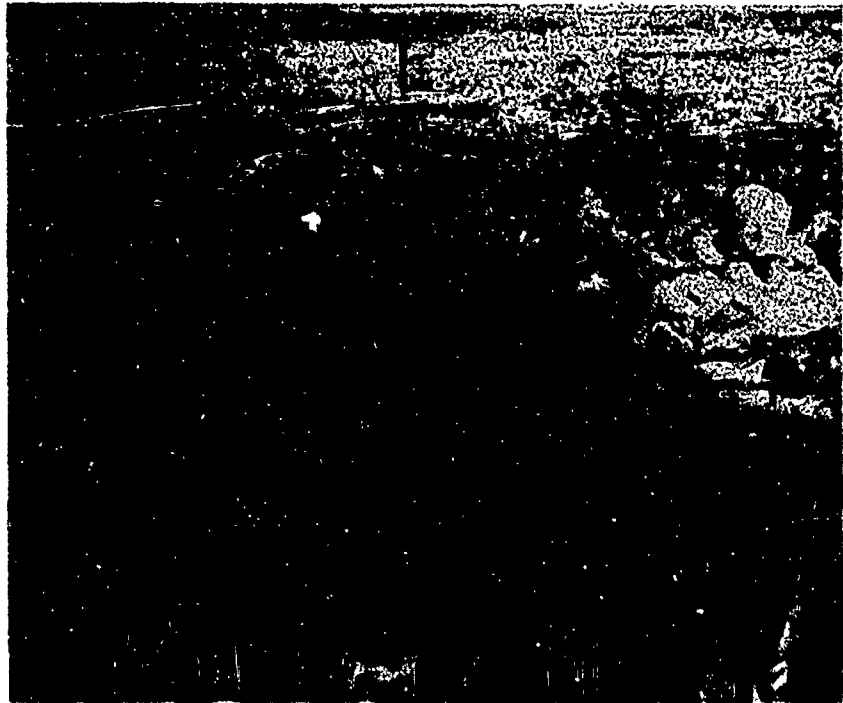


Figure 40. View of the Northwind in a rarefied ice field bursting its way through a 2-m-high ridge and fracturing a floe in its path.



Figure 41. Rarefied ice conditions around the Northwind on 13 March 1970.



Figure 42. Aerial view of the Northwind backed off from a ridge site it could not penetrate after more than an hour of ramming. The arrow indicates the point of maximum penetration. The dotted line shows the track eventually taken by the ship.

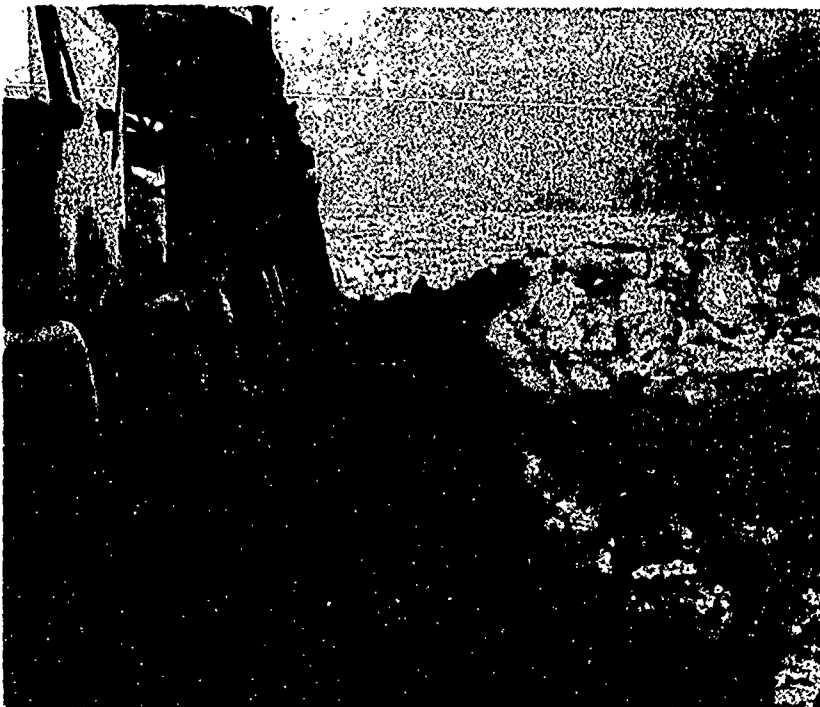


Figure 43. Ship view of ice-clogged channel and the 2-m-high ridge the Northwind attempted to penetrate.



Figure 44. Plankton (dark areas) incorporated in sea ice blocks. This photo was taken off the stern of the beset Northwind on 18 March 1970.

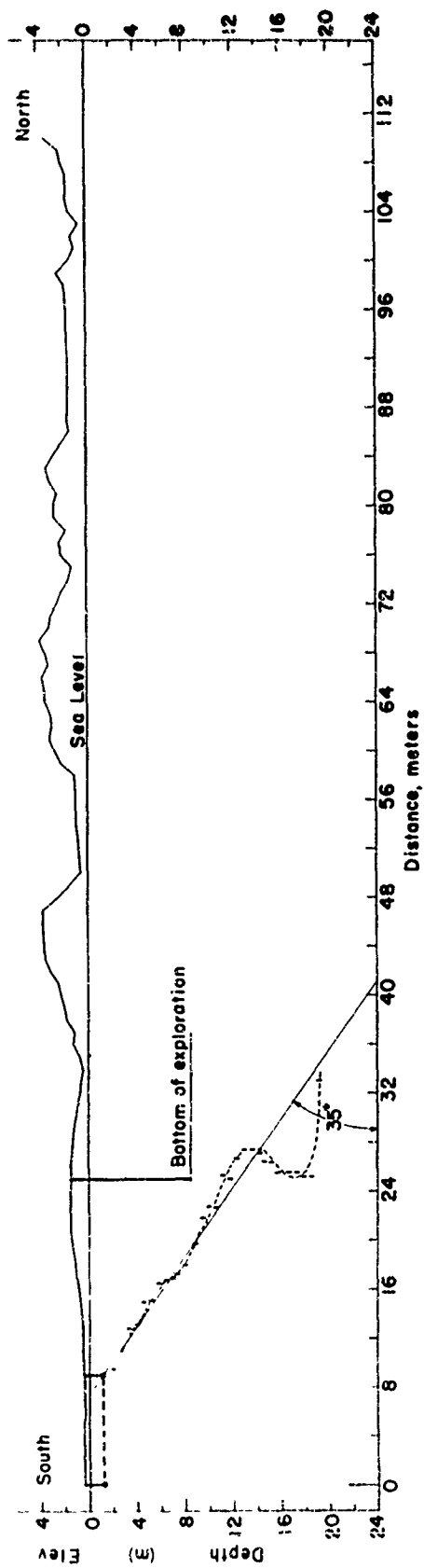


Figure 36. Profile 2B. Sonar measurements taken from station 10 M.

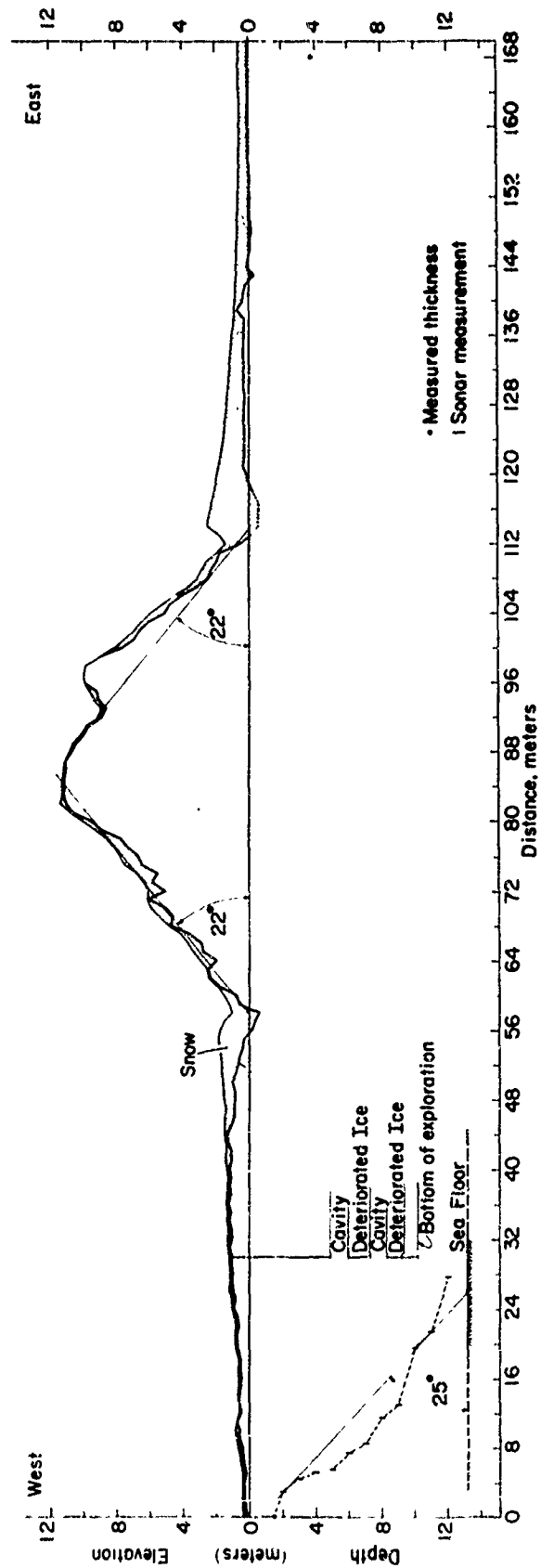


Figure 37. Profile 3. Sonar measurements taken from station 0 M.



Figure 30. Area view of the Profile 3 and 4 study site. Profile 3 was made at the ridge in the center rear (arrow points to ridge crest over which profile was made) and Profile 4 was made where the pole rests upon the ridge.

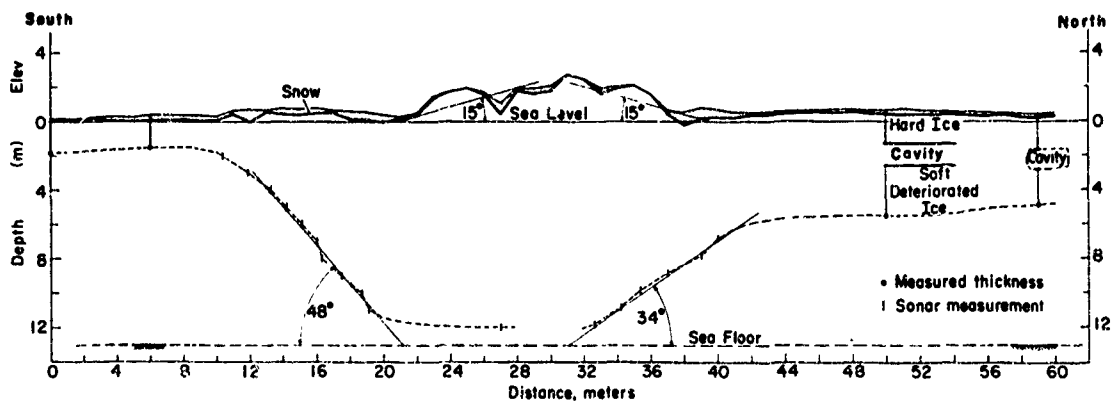


Figure 39. Profile 4. Sonar measurements taken from station 6 M and 50 M.

~~Unclassified~~  
~~Security Classification~~

DOCUMENT CONTROL DATA - R & D

(Security classification of title, body of abstract and indexing annotation must be stated when the overall report is classified)

1. ORIGINATING ACTIVITY (Corporate author) Cold Regions Research and Engineering Laboratory Corps of Engineers U.S. Army		20. REPORT SECURITY CLASSIFICATION Unclassified	
3. REPORT TITLE On the Structure of Pressure Sea Ice		25. GROUP	
4. DESCRIPTIVE NOTE (Type of report and inclusive dates)			
5. AUTHOR(S) (First name, middle initial, last name) Austin Kovacs			
6. REPORT DATE September 1970		7a. TOTAL NO. OF PAGES 57	7b. NO. OF REFS 15
8a. CONTRACT OR GRANT NO. MIPR Z-70099-02553		9a. ORIGINATOR'S REPORT NUMBER(S)	
b. PROJECT NO.		9b. OTHER REPORT NO(S) (Any other numbers that may be assigned to this report)	
c.			
d.			
10. DISTRIBUTION STATEMENT Unlimited			
11. SUPPLEMENTARY NOTES		12. SPONSORING MILITARY ACTIVITY Office of Research and Development, U.S. Coast Guard Headquarters	
13. ABSTRACT Findings presented on the geometry of several pressure-related sea ice structures, as obtained by conventional surveying and sonar profiling techniques.			

DD FORM 1 NOV 65 1473

Security Classification

KEY WORDS	LINK A		LINK B		LINK C	
	D	WT	ROLE	WT	ROLE	
Sea ice						
pressure ridges						
pressured ice						
ice structure						
surveying						
sonar						
Arctic						
Beaufort Sea						
icebreaker						